JOURNAL OF MATERIALS SCIENCE 33 (1998) 3187–3191

Structural and surface characterization of perovskite-type oxides; influence of A and B substitutions upon oxygen binding energy

C.-M. PRADIER, C. HINNEN
Laboratoire de Physico-Chimie des Surfaces, ENSCP, 11 rue P. et M. Curie 75005 Paris, France

K. JANSSON, L. DAHL, M. NYGREN
Inorganic Chemistry, Arrhenius Laboratory, Stockholm University, S-106 91 Stockholm, Sweden

A. FLODSTRÖM
Materials Physics, Royal Institute of Technology, S-100 44 Stockholm, Sweden
E-mail: pradier@ext.jussieu.fr

Monophasic samples of seven different oxides with perovskite structure, and also γ-$NaAlO_2$ have been prepared for catalytic applications. They have been characterized by X-ray diffraction and electron microscopy, then by X-ray photoelectron spectroscopy (XPS). The XPS spectra of $LaAlO_3$, $La_{0.9}Sr_{0.1}Al_{0.8}Cu_{0.1}Ru_{0.1}O_3$, $La_{0.8}Sr_{0.2}Al_{0.8}Cu_{0.1}Ru_{0.1}O_3$ and γ-$NaAlO_2$ contained only one well-defined O 1s peak. The binding energy obtained from the oxygen peak of the perovskites (529.8 eV) was, however, significantly different from that of γ-$NaAlO_2$ (532.2 eV). The other perovskite oxides, $La_{0.9}Ca_{0.1}AlO_3$, $La_{0.8}Ca_{0.2}AlO_3$, $La_{0.8}Sr_{0.2}AlO_3$ and $LaAl_{0.8}Cu_{0.2}O_3$ had two more or less well-resolved O 1s peaks separated by 2.4 eV. Tentatively, we have interpreted these observations to mean that, in the latter compounds, the surface is reconstructed so that the Al^{3+} ions have changed their coordination from octahedral to tetrahedral.

1. Introduction

The perovskite structure of the general composition ABO_3 is adopted by numerous compounds because the A and B positions can be occupied by ions having valences of A^{1+}–B^{5+}, A^{2+}–B^{4+} and A^{3+}–B^{3+} and *vice versa*. Besides the charge neutrality criterion, the radii of the A and B ions must not be too different in order for them to be accommodated in the perovskite framework. In addition, a proper combination of cations can stabilize anion vacancies in the perovskite framework, and unusual formal oxidation states of the metal ions can be obtained. The ideal perovskite is cubic, but distorted modifications having rhombohedral (hexagonal) symmetry are frequently occurring. The A ions in ABO_3 are coordinated by 12 oxygen atoms, while the coordination sphere around the B ions is octahedral. These structural features make it possible to tailor the chemical and physical properties of compounds possessing perovskite-based structures.

In catalytic applications pseudo-binary and ternary perovskite-based oxides of the composition ABO_3 and $A_{1-x}A'_xBO_3$, respectively, have been most frequently studied [1–4] but a few studies concerning the catalytic behaviour of pseudo-quaternary compounds, such as $A_{1-x}A'_xB_{1-y}B'_yO_3$ can be found [5, 6]. Recently, Skoglundh *et al.* [7] and Teraoka *et al.* [8] have reported on the catalytic properties of a pseudo-quinary perovskite of an entirely new composition $La_{1-x}Sr_xM_{1-2y}Cu_yRu_yO_3$, with M = Al or Co. The compounds with M = Al were found to be catalytically active for simultaneous reduction of NO and oxidation of CO and C_3H_6, while the compounds with M = Co mainly behaved as oxidative catalysts.

Assuming that the redox abilities of these oxides are closely related to the electronic structure of the surface oxygen and cations, we performed *in situ* photoelectron spectroscopy (XPS) analysis of $La_{1-x}Sr_xM_{1-2y}Cu_yRu_yO_3$ samples ($x = 0.2$ and $0 \leqslant y \leqslant 0.2$) to gain more insight into the electronic state of these oxide surfaces. X-ray photoelectron spectroscopy (XPS) results for several samples are presented here in order to draw some tendencies regarding the role of the nature of the substituted cation. The binding energy of oxygen and the valence states of metal ions involved have been carefully determined. The XPS spectra of some of the compounds contained, in particular, two O 1s peak revealing a 2.3 eV difference in binding energies (BE).

In this paper we report on XPS studies of seven perovskite compounds of the compositions $LaAlO_3$, $La_{0.9}Ca_{0.1}AlO_3$, $La_{0.8}Ca_{0.2}AlO_3$, $La_{0.8}Sr_{0.2}AlO_3$, $LaAl_{0.8}Cu_{0.2}O_3$, $La_{0.9}Sr_{0.1}Al_{0.8}Cu_{0.1}Ru_{0.1}O_3$ and

0022–2461

$La_{0.8}Sr_{0.2}Al_{0.8}Cu_{0.1}Ru_{0.1}O_3$. In addition, we have prepared γ-$NaAlO_2$, which has a tetragonal unit cell with aluminium ions tetrahedrally coordinated by oxygen, and report its XPS spectrum. All samples studied were monophasic according to their X-ray powder patterns. Special attention is paid to the occurrence of one or two O 1s peaks, which appear when, due to appropriate substitution, there should be anion vacancies in the bulk of the perovskite framework, and the B ions located at the surface can be expected to change their coordination from octahedral to tetrahedral.

2. Experimental procedure

2.1. Sample preparation, X-ray diffraction and SEM–TEM characterization

The following starting materials (all of *p.a.* quality) have been used; $La(NO_3)_3 \cdot 6H_2O$ (Kebo AB), $Sr(NO_3)_2$ (Merck), $Ca(NO_3) \cdot 4H_2O$ (Kebo AB), $Al(NO_3)_3 \cdot 9H_2O$ (Merck), $Cu(NO_3)_2 \cdot 3H_2O$ (Merck), $RuCl_3$ (Johnson Matthey), Al_2O_3 (Kebo AB) and Na_2CO_3 (Merck).

Appropriate amounts of the metal salts were dissolved in deionized water to form solutions with compositions corresponding to the metal content in the following compounds, $LaAlO_3$, $La_{0.9}Ca_{0.1}AlO_3$, $La_{0.8}Ca_{0.2}AlO_3$, $La_{0.8}Sr_{0.2}AlO_3$, $LaAl_{0.8}Cu_{0.2}O_3$, $La_{0.9}Sr_{0.1}Al_{0.8}Cu_{0.1}Ru_{0.1}O_3$ and $La_{0.8}Sr_{0.2}Al_{0.8}Cu_{0.1}Ru_{0.1}O_3$. The solutions were then evaporated to dryness under stirring and the residues were calcined in air at 820 K for 1 h. The oxide mixtures thus formed were pelletized and isothermally heat treated in air at 1270 K for 2 wk ($La_{0.9}Sr_{0.1}Al_{0.8}Cu_{0.1}Ru_{0.1}O_3$ and $La_{0.8}Sr_{0.2}Cu_{0.1}Ru_{0.1}O_3$) or at 1570 K for 36 h ($LaAlO_3$, $La_{0.9}Ca_{0.1}AlO_3$, $La_{0.8}Ca_{0.2}AlO_3$, $La_{0.8}Sr_{0.2}AlO_3$, $LaAl_{0.8}Cu_{0.2}O_3$).

γ-$NaAlO_2$ was prepared by mixing appropriate amounts of Na_2CO_3 and Al_2O_3 and then heat treating the mixture at 1170 K for 2 h. This mixture was then pelletized and heat treated at 1370 K for 24 h.

The X-ray powder patterns of the prepared samples were obtained in a Guinier Hägg camera using Cu$K\alpha_1$ radiation. Silicon was added to the samples as internal standard and the powder diffractograms were evaluated with a film scanner system [9]. The lattice parameters were found by use of an upgraded version of the program PIRUM [10] and the obtained records were matched with tabulated JCPDS data.

The surface morphology of the materials, and the element compositions of individual grains were studied in a scanning electron microscope (SEM, Jeol 820) and an analytical transmission electron microscope (ATEM, Jeol 2000 FX), both equipped with energy-dispersive spectrometers (EDS, LINK AN 10000). The samples used in the TEM/EDS studies were prepared by transferring powder on to a perforated carbon film supported by a nickel grid.

2.2 Surface characterization

A VG Escalab Mark II spectrometer was used in these experiments. The instrument is equipped with a preparation chamber in which the samples were treated in pure oxygen, $P = 10^{-6}$ torr (1 torr = 133.322 Pa), at $T = 1073$ K for 1 h, before being transferred to the XPS chamber where the base pressure was equal to 8×10^{-10} torr. In order to avoid water deposition during cooling, the sample was cooled before oxygen evacuation. MgK_α radiation (1253.6 eV) was used as excitation source with a constant pass energy of 20 eV for high-resolution spectra and 50 eV for wide scans.

The samples were pressed into 2 mm thick pellets and mounted on a gold foil maintained with gold strips. The gold foil is used for internal calibration of the spectrometer using a binding energy of 83.9 eV for Au $4f_{7/2}$. Correction for charge effects was achieved by referring to an internal standard. La $3d_{5/2}$ at 834.2 eV was used for all samples containing La and Na 1s at 1073.1 eV for $NaAlO_2$.

3. Results

3.1. Phase analysis and SEM-ATEM/EDS studies

The samples prepared as described above were all monophasic according to their X-ray powder pattern. The cell parameters of γ-$NaAlO_2$, $a = 0.531\,87(2)$ and $c = 0.707\,08(3)$ nm, are in good agreement with those given elsewhere [11]. The diffractograms of the samples with perovskite structure could be indexed with use of a hexagonal ($LaAlO_3$) and/or cubic unit cell and the cell parameters are given in Table I.

The SEM-EDS studies showed that the overall metal compositions of the samples were in good agreement with the nominal ones. The ATEM-EDS studies showed that the individual grains had a metal composition close to that given by their chemical formula.

3.2. XPS studies

3.2.1. O 1s binding energy

All oxides were analysed after heat treatment in oxygen. This treatment was assumed to eliminate water and hydroxyl contamination. The main features of the spectra are as follows:

(i) a single main peak for $LaAlO_3$, $La_{0.9}Sr_{0.1}Al_{0.8}Cu_{0.1}Ru_{0.1}O_3$, $La_{0.8}Sr_{0.2}Al_{0.8}Cu_{0.1}Ru_{0.1}O_3$ at 530 ± 0.2 eV and for γ-$NaAlO_2$ at 532.2 ± 0.1 eV;

(ii) a more complex oxygen structure for all other oxides, $La_{0.9}Ca_{0.1}AlO_3$, $La_{0.8}Ca_{0.2}AlO_3$, $La_{0.8}Sr_{0.2}AlO_3$ and $LaAl_{0.8}Cu_{0.2}O_3$. The O 1s line could be fitted with a major low binding energy (LBE) contribution at 529.8/529.9 eV associated with a high binding energy (HBE) contribution at 532.2 eV.

TABLE I Unit cell parameters of the prepared perovskite samples

Sample	a_{cub}(nm)	a_{hex}(nm)	c_{hex}(nm)
$LaAlO_3$	0.379 21(2)	0.536 31(4)	1.311 7(2)
$La_{0.9}Ca_{0.1}AlO_3$	0.378 98(3)		
$La_{0.8}Ca_{0.2}AlO_3$	0.378 74(2)		
$La_{0.8}Sr_{0.2}AlO_3$	0.379 41(4)		
$LaAl_{0.8}Cu_{0.2}O_3$	0.379 24(3)		
$La_{0.9}Sr_{0.1}Al_{0.8}Cu_{0.1}Ru_{0.1}O_3$	0.379 99(4)		
$La_{0.8}Sr_{0.2}Al_{0.8}Cu_{0.1}Ru_{0.1}O_3$	0.380 65(5)		

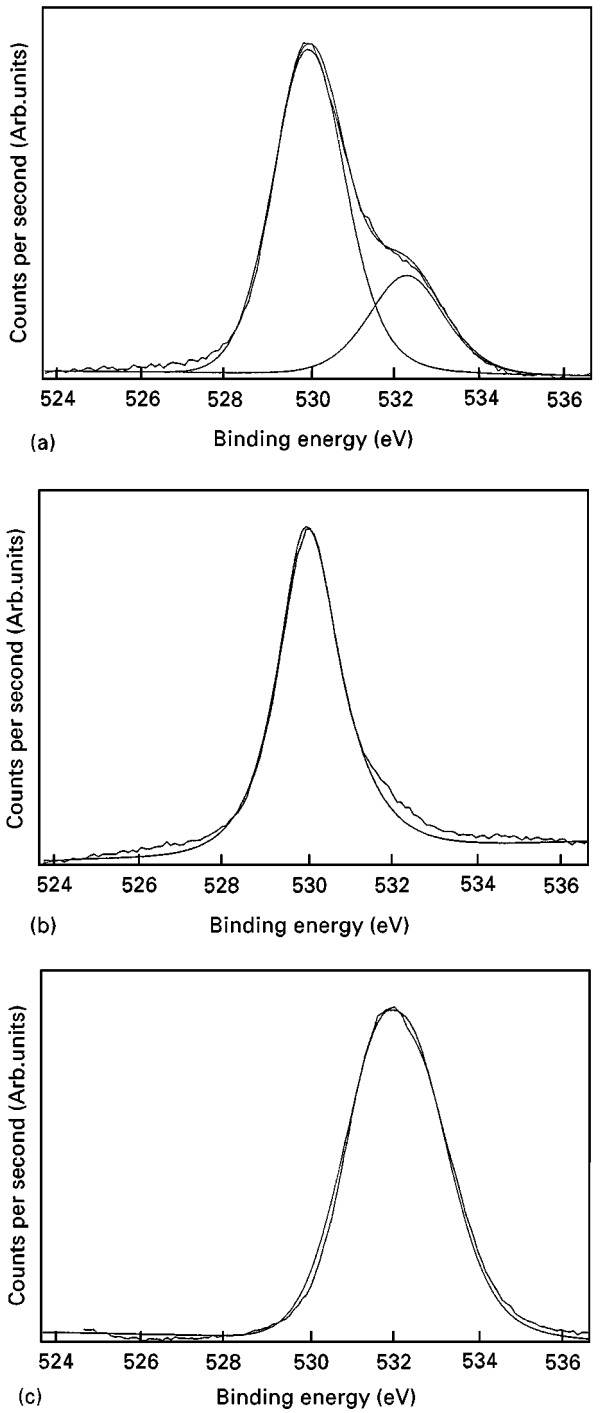

Figure 1 O 1s core level spectra of (a) $La_{0.8}Ca_{0.2}AlO_3$ showing two separate O 1s components centred at 529.8 and 532.2 eV, and of (b) $LaAlO_3$ and (c) $NaAlO_2$ with O 1s positions centred at 529.9 and 532.2 eV, respectively.

The high resolution O 1s spectra for $LaAlO_3$, $NaAlO_2$ and for one representative compound exhibiting the two oxygen contributions are given in Fig. 1. The observed oxygen peak binding energies, for all investigated samples, are given in Table II.

A test experiment was performed with one of the "double-oxygen" samples, $La_{0.8}Ca_{0.2}AlO_3$ in order to make sure that the high BE peak can be assigned to a bound state. The sample was left in the air at RT for one night, then heat treated again in oxygen at 1073 K with XPS analyses in between. The resulting O 1s spectra are shown in Fig. 2: contact with the air gives rise to an increase of the O 1s contribution at 532.2 eV, then after heating in oxygen to decrease down to the level observed in Fig. 1. This test makes it clear that the high BE contribution can originate from two different oxygen species, one ascribed to OH or H_2O reversibly absorbed in the air and eliminated by heating, the other one being intrinsic to the oxide surface structure.

Conversely to the low BE peak for which fitting parameters are identical for all samples (FWHM = 1.6 eV), the FWHM of the high BE peaks could not be maintained at a constant value for the fitting procedures. The width of the O 1s peak for γ-$NaAlO_2$ is notable; it could be fitted with only one contribution having a FWHM of 2.5 eV. This is likely to be due to environmental effects.

It is remarkable that the two oxygen peaks are located at very similar binding energies in all oxides, i.e. 530.0 ± 0.2 and 532.2 ± 0.1 eV. It is also worthwhile to note that the ratio of the intensities of the high binding-energy (HBE) peak and the low one (LBE) is very close to 1/4 in the spectra containing two O 1s peaks (ranging from 11/89 to 25/75, see Table II).

3.2.2. Cation binding energies

The binding energies of the La $3d_{5/2}$, Cu $2p_{3/2}$, Al 2s, Sr $3d_{5/2}$, Ca $2p_{3/2}$ and Na 1s levels of the prepared oxides are given in Table II. The XPS spectrum of $LaAl_{0.8}Cu_{0.2}O_3$ has no shake-up satellite peaks in the Cu $2p_{3/2}$ region as shown in Fig. 3. The same observation was made for the two other oxides containing copper. In lanthanum-containing oxides, the La XPS $3d_{3/2}$ and $3d_{5/2}$ core levels are split into two components of comparable intensities, as previously found [12]; see, as an example, the La $3d_{5/2}$ levels of $LaAl_{0.8}Cu_{0.2}O_3$ in Fig. 3. It can also be noted that, throughout this series of oxides, the binding energy of the Al 2s peak varies significantly with the composition of the sample. Note that the aluminium peaks, 2s or 2p levels, are small and not well enough defined to enable a description and a fitting procedure. Strontium and calcium core-level peaks are, however, observed at the expected binding energies for $Sr^{2+}(3d_{5/2})$ and $Ca^{2+}(2p_{3/2})$ cations, respectively, in all compounds. Table II does not contain any binding energies for the Ru 3d levels, as these XPS peaks cannot be easily identified because they are partially overlapped by the Sr 3p peaks and because ruthenium is likely to exhibit several valence states, which in turn broadens the Ru 3d levels.

It can be noted that the use of the La $3d_{5/2}$ and Na 1s peaks as internal standards led to a consistent set of binding energies of oxygen and of all cations except Al^{3+} as mentioned above.

No trace of impurities could be detected by XPS in any sample; even the level of carbon was very low (C 1s intensity never exceeds 1/10 of the O 1s one).

4. Discussion

The main observations are as follows:

(i) all samples are monophasic;

(ii) the variation of the lattice parameters of the unit cell of the perovskite phases with composition can be ascribed to ion radius differences between the substituting and the host ones;

TABLE II Binding energies of the main XPS lines

Sample	O 1s (eV)		I_{HBE}/I_{LBE}	La $3d^a_{5/2}$ (eV)	Cu $2p_{3/2}$ (eV)	Ca $2p_{3/2}$ (eV)	Na 1s[a] (eV)	Al 2s (eV)	Sr $3d_{5/2}$ (eV)
	LBE	HBE							
$LaAlO_3$	529.9			834.2				119.4	
$LaAl_{0.8}Cu_{0.2}O_3$	529.9	532.1	11/89	834.2	932.6			117.4	
$La_{0.8}Sr_{0.2}AlO_3$	529.8	532.2	25/75	834.2				118.4	134.1
$La_{0.9}Sr_{0.1}Al_{0.8}Cu_{0.1}Ru_{0.1}O_3$	529.8			834.2				117.9	134.0
$La_{0.8}Sr_{0.2}Al_{0.8}Cu_{0.1}Ru_{0.1}O_3$	530.2			834.2				118.2	133.9
$La_{0.9}Ca_{0.1}AlO_3$	529.8	532.2	20/80	834.2		347.4		118.4	
$La_{0.8}Ca_{0.2}AlO_3$	529.8	532.2	19/81	834.2		347.5		118.1	
$NaAlO_2$		532.2					1073.1	119.2	

[a] Internal standards.

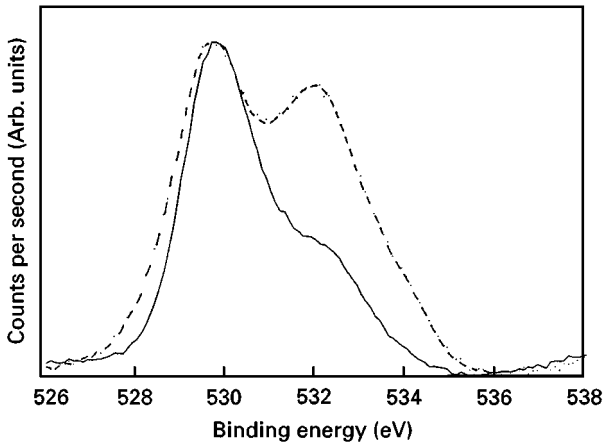

Figure 2 Influence of heating treatment on the O 1 XPS spectra of $La_{0.8}Ca_{0.2}AlO_3$: (—) after annealing treatment at 1073 K in an O_2 atmosphere, (- - -) after being left in air.

(iii) the splitting of the La $3d_{3/2}$ and $3d_{5/2}$ core levels is a well-known phenomenon observed for rare-earth ionic compounds with low Z-values, e.g. in La_2O_3 [12]. It has been interpreted in terms of an interaction of the valence band of the solid and the f-states of the lanthanum ion in the final state of photoionization. Another interpretation, based on a quantitative description of core hole screening populations, is given elsewhere [13];

(iv) the perovskite-based oxides $La_{0.9}Ca_{0.1}AlO_3$, $La_{0.8}Ca_{0.2}AlO_3$, $La_{0.8}Sr_{0.2}AlO_3$ and $LaAl_{0.8}Cu_{0.2}O_3$ have two separated O 1s peaks with binding energies equal or very close to those of the two "simple" oxides $LaAlO_3$ and $NaAlO_2$;

(v) the perovskite-based oxides $La_{0.9}Sr_{0.1}Al_{0.8}Cu_{0.1}Ru_{0.1}O_3$ and $La_{0.8}Sr_{0.2}Al_{0.8}Cu_{0.1}Ru_{0.1}O_3$ have one O 1s peak with the same binding energy as that found for $LaAlO_3$;

(vi) we note fluctuating values of the binding energies for the Al 2s level which may indicate that the oxygen environments around the Al^{3+} ions are different in these samples, and/or that electron transfer to the Al^{3+} ions takes place;

(vii) in the three copper-containing oxides, no satellite could be observed to the Cu 2p peak, suggesting monovalent state for copper cations in these oxides.

The absence of satellite to the Cu 2p line deserves further discussion in the light of two recent review papers reporting photoemission signals and their interpretations for high-quality surfaces of high-temperature superconductors, by Vasquez [14] and Parmigiani and Sangaletti [15], respectively. High-quality cuprate superconductors should be characterized by a Cu 2p signal with the complex satellite characteristic of the 2 + oxidation state and, the O 1s peak is at 529 eV, with negligible signal above 531 eV. This seems rather contradictory to our results. But, the samples, studied here, are not cuprates. The complexity of the structure of these oxides does not permit a clear prediction of the oxidation state and hybridization mechanism of copper. Moreover charge compensation may occur in these multisubstituted oxides. In particular, the enrichment of oxygen around

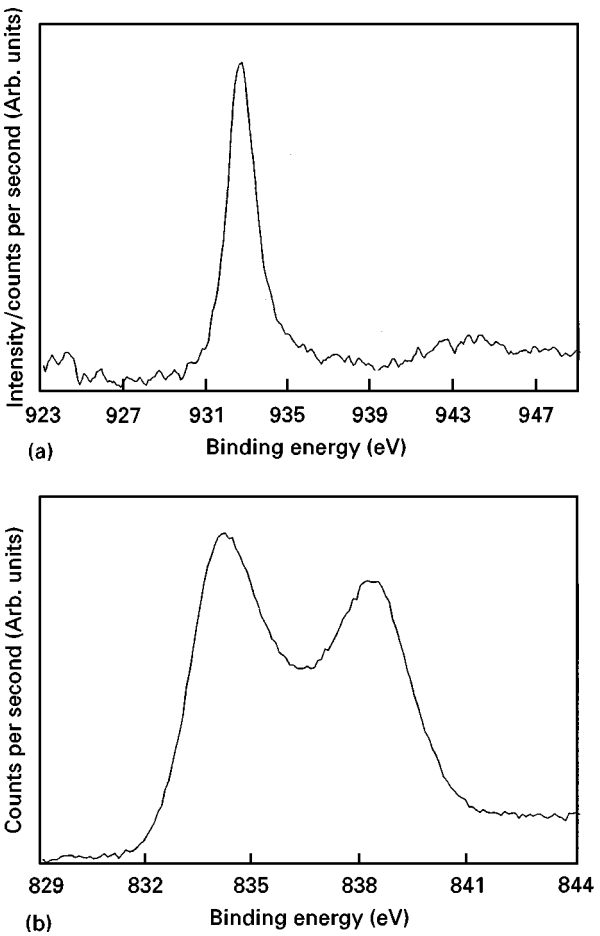

Figure 3 High-resolution XPS spectra of (a) Cu $2p_{3/2}$ and (b) La $3d_{5/2}$ of $LaAl_{0.8}Cu_{0.2}O_3$, showing the absence of the satellite peak characteristic of CuO and the splitting of the La $3d_{5/2}$ peak.

aluminium cations could be correlated to a local oxygen deficiency around copper ions, consistent with the Cu^+ oxidation state.

The different O 1s binding energies observed for $LaAlO_3$ (529.9 eV) and $NaAlO_2$ (532.2 eV) are remarkable. The low-energy O 1s peak is characteristic for an oxy-ion in an oxide lattice. The high-energy O 1s peak is not common for oxides. We do not ascribe the latter peak to hydroxide or to adsorbed water, because all oxides have been heated in oxygen at 1073 K before the XPS analysis. This treatment should remove all H_2O or OH groups. Moreover, OH groups "grow" at the surface in the air leading to the increase in the peak intensity at 532.2 eV. The peak at high BE, left after heat treatment at 1073 K and cooling in high vacuum, is specific to the oxide structure.

The existence of an oxygen bounded to the oxide, and giving rise to a O 1s at high BE, was first mentioned by Parmigiani *et al.* to explain a high BE O 1s peak observed for 2212 single crystals of bismuth-based superconductors [16]. It was also observed by Hinnen *et al.* in an XPS study of $Bi_2Sr_2CaCu_2O_{8+\delta}$ oxides [17].

The photoemission data suggest that charge neutrality requirements in these compounds are, to a great extent, fulfilled by oxygen vacancies rather than by a cation charge compensation mechanism. In order to fulfil the charge neutrality criteria it is thus most probable that $La_{0.9}Ca_{0.1}AlO_3$, $La_{0.8}Ca_{0.2}AlO_3$, $La_{0.8}Sr_{0.2}AlO_3$ and $LaAl_{0.8}Cu_{0.2}O_3$ contain more anion vacancies than $La_{0.9}Sr_{0.1}Al_{0.8}Cu_{0.1}Ru_{0.1}O_3$ and $La_{0.8}Sr_{0.2}Al_{0.8}Cu_{0.1}Ru_{0.1}O_3$ do, as the latter compounds contain an ion (Ru) which can easily adjust its valence state.

Tentatively we have thus interpreted these observations so that when the anion vacancy concentration is large enough, a reconstruction of the surface occurs and this reconstruction implies a change of the coordination of the Al^{3+} ions from octahedral to tetrahedral. The surface structural modification ascribed to oxygen deficiency is compatible with the treatment in oxygen at 700 °C; in fact, at that temperature, oxygen can clean the surface but not induce any restructuring.

Preliminary calculations have revealed a difference of about 3 eV in the O 1s binding energies for Al^{3+} in octahedral and tetrahedral configuration. Molecular dynamic calculations have shown that the structure of the surface of $LaAlO_3$ at 300 K is reorganized in such a way that the oxygen concentration in the superficial layer is higher than in the bulk material, resulting in a change in Al^{3+} coordination from octahedral to tetrahedral [18]. These preliminary results support our interpretation of the obtained XPS spectra even though we have not observed a reconstruction of the surface of $LaAlO_3$ itself, but for a corresponding perovskite doped on the A and B positions. The occurrence of two components for O 1s has already been mentioned by Berchner *et al.* to occur in $YBa_2Cu_3O_{7-\delta}$ thin films at very similar BE, 528.5 and 530.7 eV [19]. The same authors also report a LEED characterization of this oxide, which led them to ascribe the two states of oxygen to the formation of a superstructure which stabilizes the surface under vacuum. It can also be noted that the high-BE O 1s satellite peak in high T_c oxide superconductors has been attributed to oxygen ions adsorbed on the surface of the sample [20]. Temperature-programmed oxygen desorption studies of (La,M)-Co-based perovskites with M = Ca or Sr have shown that all adsorbed oxygen ions leave the sample at temperatures below approximately 970 K [8, 21].

Samples where the A and B ions in $LaAlO_3$ are replaced by other ions and $LaGaO_3$ doped with various metal ions, are presently being prepared. The results of these experiments together with the calculations briefly described above will be presented in a forthcoming article.

Acknowledgements

This work has been financially supported by the Swedish National Research Council and by the Swedish Board for Industrial Technical Development. The contribution of J. M. Siffre in connection with the XPS measurements is gratefully acknowledged.

References

1. R. J. H. VOORHOEVE, in "Advanced Materials in Catalysis", edited by J. J. Burton and R. L. Garten (Academic Press, New York, 1977) p. 129.
2. L. G. TEJUCA, J. L. G. FIERRO and J. M. D. TASCON, *Adv. Catal.* **36** (1989) 237.
3. M. MISONO and E. A. LOMBARDO (eds), "Perovskites, A special issue of Catalysis Today", Vol. 8, no. 2 (Elsevier, Amsterdam, 1990).
4. L. G. TEJUCA, J. L. G. FIERRO (eds), "Perovskite Oxides, A special issue of Catalysis Reviews", Vol. 34, no. 4 (Marcel Dekker, New York, 1992).
5. H. M. ZHANG, Y. SHIMIZU, Y. TERAOKA, N. MIURA and N. YAMAZOE, *J. Catal.* **121** (1990) 432.
6. D. KLVANA, J. VAILLANCOURT, J. KIRCHEROVA and J. CHAOKI, *Appl. Catal. A* **109** (1994) 181.
7. M. SKOGLUNDH, L. LÖWENDAHL, K. JANSSON, L. DAHL and M. NYGREN, *Appl. Catal. B* **3** (1994) 259.
8. Y. TERAOKA, H. NII, S. KAGAWA, K. JANSSON and M. NYGREN, *J. Mater. Chem.* **6** (1996) 97.
9. K. E. JOHANSSON, T. PALM and P. E. WERNER, *J. Phys. E* **13** (1980) 1289.
10. P. E. WERNER, *Arkiv Kemi* **31** (1969) 513.
11. JCPDS 19-1179 (Joint Committee for Powder Diffraction Studies Swathmore, PA).
12. K. JÖRGENSEN and H. BERTHOU, *Chem. Phys. Lett.* **13** (1972) 186.
13. W. D. SCHNEIDER, B. DELLEY, E. WUILLOUD, J. M. IMER and Y. BAER, *Phys. Rev. B* **32** (1985) 6819.
14. R. P. VASQUEZ, *J. Electron Spectrosc. Relat. Phenom.* **66** (1994) 209.
15. F. PARMIGIANI and L. SANGALETTI, *ibid.* **66** (1994) 223.
16. F. PARMIGIANI, Z. X. SHEN, D. B. MITZI, I. LINDAU, W. E. SPICER and A. KAPITULNIK, *Phys. Rev. B* **43** (1991) 3085
17. C. HINNEN, C. NGUYEN VAN HUONG, P. MARCUS, *J. Electron Spectrosc. Relat. Phenom.* **73** (1995) 293
18. L. PETTERSSON and K. HERMANSSON, private communication (1975).
19. H. BERCHNER, K. RÜHRNSCHOPF, W. RAUCH and G. WEDLER, *Appl. Surf. Sci.* **68** (1993) 179.
20. P. STEINER, R. COURTHS, V. KINSINGER, I. SANDER, B. SIEGWART and S. HUFNER, *Appl. Phys. A* **44** (1987) 7.
21. Y. TERAOKA, M. YOSHIMATSU, N. YAMAZOE and T. SEIYAMA, *Chem. Lett.* (1984) 893.

Received 21 October 1996
and accepted 18 March 1998